High-Temperature Chemical and Microstructural Transformations of a Nanocomposite Organoceramic

Phillip B. Messersmith† and Samuel I. Stupp*

Departments of Materials Science and Engineering and Chemistry, Beckman Institute for Advanced Science and Technology and Materials Research Laboratory, University of Illinois at Urbana–Champaign, Urbana, Illinois 61801

Received April 20, 1994. Revised Manuscript Received December 9, 1994®

This paper describes the microstructural and chemical transformations occurring at high temperatures in polymer/inorganic crystal nanocomposites referred to as organoceramics. The organoceramic investigated consists of alternating layers of poly(vinyl alcohol) (PVA) and the layered double hydroxide $[Ca_2Al(OH)_6]^+[(OH)\cdot 3H_2O]^-$, with a structural repeat distance of approximately 18 Å. The nanocomposite was heated to various temperatures up to 1000 °C and analyzed using X-ray diffraction, infrared spectroscopy, thermogravimetric analysis, scanning electron microscopy, and chemical analysis. The layered structure of the organoceramic was found to be stable up to a temperature of 400 °C, whereas the pure layered double hydroxide lacking organic material decomposed at 125 °C. The high thermal stability of the organoceramic nanocomposite may arise from an extensive and strongly bonded interface between organic and inorganic components. Interestingly, the organoceramic heated to 1000 °C transforms into an inorganic solid which has a different phase composition than the layered double hydroxide heated to the same temperature.

Introduction

The realization that a nanoscale dispersion of phases in composite materials can impact profoundly on physical properties has led to the search for new synthetic pathways for such materials. These materials are referred to as nanocomposites and can take many forms that usually exhibit interesting physical properties often as a result of their ultrafine microstructure.[1] In our laboratory we developed a synthetic pathway involving the nucleation and growth of inorganic phases in solutions of ion-binding polymers or polyelectrolytes.[2–6] These materials were labeled organoceramics since their synthetic pathway led naturally to molecularly dispersed polymer molecules in the inorganic lattice. One specific system[4–6] involved the intercalation of polymers between the inorganic nanolayers of calcium aluminates. Other layered inorganic materials have been found to be suitable for nanocomposite synthesis because of their ability to act as hosts for polymer intercalation or as templates for the polymerization of intercalated monomer.[7–17] Our synthetic approach is unique in that a preexisting layered host is not used, rather, spontaneous self-assembly of the inorganic and organic phases from homogeneous aqueous solution results in formation of the layered nanocomposite.[4]

Self-assembly is ubiquitous in nature and involves the spontaneous aggregation of molecules into stable, well-ordered structures. Related to this is the concept of synthesis of new polymer/ceramic composite materials via the molecular self-assembly of macromolecules within a ceramic crystal lattice during crystal growth, with the expectation of obtaining hybrid materials that combine the properties of ceramics and polymers. Recently, it has been demonstrated that biogenic macromolecules extracted from the mineralized shells of certain marine organisms can be occluded within the lattice of $CaCO_3$ crystals grown in the laboratory.[18–20] Furthermore, when compared to pure synthetic $CaCO_3$ crystals, the modified crystals (and their biogenic analogues) exhibit unique fracture properties. Recent

† Current address: Department of Restorative Dentistry, University of Illinois at Chicago, Chicago, IL 60612.
* To whom correspondence should be addressed.
® Abstract published in *Advance ACS Abstracts,* January 15, 1995.

(1) Komarneni, S. *J. Mater. Chem.* **1992**, *2*, 1219.
(2) Stupp, S. I.; Ciegler, G. W. *J. Biomed. Mater. Res.* **1992**, *26*, 169.
(3) Stupp, S. I.; Mejicano, G. C.; Hanson, J. A. *J. Biomed. Mater. Res.* **1993**, *27*, 289.
(4) Messersmith, P. B.; Stupp, S. I. *J. Mater. Res.* **1992**, *7*, 2599.
(5) Messersmith, P. B.; Stupp, S. I. In *Advanced Cementitious Systems: Mechanisms and Properties*; Glasser, F. P., Pratt, P. L., Mason, T. O., Young, J. F., McCarthy, E. G., Eds.; *Mat. Res. Soc. Symp. Proc.* **1992**, *245*, 191.
(6) Messersmith, P. B.; Stupp, S. I. *Polym. Prepr.* **1991**, *32*, 536.
(7) For recent reviews on nanocomposites based on layered solids, see: Komarneni, S. *J. Mater. Chem.* **1992**, *2*, 1219. Ozin, G. A. *Adv. Mater.* **1992**, *4*, 612. Lagaly, G. In *Developments in Ionic Polymers;* Wilson, A. D., Prosser, H. J., Eds.; Elsevier: London, 1986; Vol. II, p 77. Ruiz-Hitzky, E. *Adv. Mater.* **1993**, *5*, 334 and references therein.
(8) Kanatzidis, M. G.; Marcy, H. O.; McCarthy, W. J.; Kannewurf, C. R.; Marks, T. J. *Solid State Ionics* **1989**, *32/33*, 594.
(9) Kanatzidis, M. G.; Wu, C.-G.; Marcy, H. O.; Kannewurf, K. R. *J. Am. Chem. Soc.* **1989**, *111*, 4139.
(10) Messersmith, P. B.; Giannelis, E. P. *Chem. Mater.* **1993**, *5*, 1064.
(11) Ruiz-Hitzky, E.; Aranda, P. *Adv. Mater.* **1990**, *2*, 545.
(12) Aranda, P.; Ruiz-Hitzky, E. *Chem. Mater.* **1992**, *4*, 1395.
(13) Mehrotra, V.; Lombardo, S.; Thompson, M. O.; Giannelis, E. P. *Phys. Rev. B* **1991**, *44*, 5786.
(14) Divigalpitiya, W. M. R.; Frindt, R. F.; Morrison, S. R. *J. Mater. Res.* **1991**, *6*, 1103.
(15) Fukushima, Y.; Okada, A.; Kawasumi, M.; Kurauchi, T.; Kamigaito, O. *Clay Miner.* **1988**, *23*, 27.
(16) Kato, C.; Kuroda, K.; Misawa, M. *Clays Clay Miner.* **1979**, *27*, 129.
(17) Blumstein, A. *J. Polym. Sci., Part A* **1965**, *3*, 2653.
(18) Berman, A.; Addadi, L.; Weiner, S. *Nature* **1988**, *331*, 546.
(19) Berman, A.; Addadi, L.; Kvick, A.; Leiserowitz, L.; Nelson, M.; Weiner, S. *Science* **1990**, *250*, 664.
(20) Berman, A.; Hanson, J.; Leiserowitz, L.; Koetzle, T. F.; Weiner, S.; Addadi, L. *Science* **1993**, *259*, 776.
(21) Pritchard, J. G. *Poly(Vinyl Alcohol)*, Gordon and Breach: New York, 1972.
(22) Allmann, R. *Chimia* **1970**, *24*, 99.

0897-4756/95/2807-0454$09.00/0

work suggests that control of crystal texture in this manner may be common practice among organisms that produce mineralized tissue, as a means of adapting tissue structure to function.[20]

We have utilized a similar self-assembly approach to synthesize the polymer–ceramic nanocomposites we call organoceramics. These materials contain as much as 50% polymer by weight yet retain a molecular-scale dispersion of polymer within a layered crystalline ceramic phase. The synthesis of organoceramic is unique and unlike the polymer intercalation compounds described above. In organoceramics formation of the inorganic layered phase from ionic precursors occurs simultaneously with the assembly of polymer into intervening layers of thickness on the order of 10 Å.[4] These organoceramic materials may have a wide range of applications in areas such as structural materials, hydraulic cements, and biomaterials. The specific materials investigated are those resulting from the aqueous precipitation of the layered double hydroxide (LDH) $[Ca_2Al(OH)_6]^+[(OH)\cdot 3H_2O]^-$ in the presence of dissolved poly(vinyl alcohol) (PVA). The structure of the product consists of LDH layers separated by interlayers containing anions, PVA, and water. In the layered nanocomposite, the observed layer spacing expands from 7.8 Å, the spacing of the pure LDH, to approximately 18 Å as a result of polymer intercalation between inorganic layers. The mechanism of polymer intercalation is believed to involve nucleation and growth of calcium aluminate layers by the polymer as well as polymer adsorption.[4] Preliminary experiments involving the PVA organoceramic suggested an enhanced thermal stability in the nanocomposite relative to that of individual components.[5] The purpose of this paper is to report a more complete analysis of the chemical, structural, and morphological changes occurring when the organoceramic is exposed to elevated temperatures. In this work, thermally induced transformations in the PVA organoceramic were probed by X-ray diffraction (XRD), scanning electron microscopy (SEM), Fourier transform infrared spectroscopy (FTIR), thermogravimetric analysis (TGA), and chemical analysis.

Experimental Section

The synthesis of the PVA organoceramic and the layered double hydroxide (LDH) was accomplished by mixing a calcium hydroxide/polymer solution with a solution containing calcium and aluminum hydroxides.[4] The calcium hydroxide solution was prepared by stirring excess CaO (Alfa Chemicals, Ward Hill, MA) in 1–2 L of deionized water at 5 °C. Both solutions were filtered to remove solid particles, yielding clear ionic solutions. Under these conditions the concentration of the calcium hydroxide solution was 25 mM, whereas the calcium aluminate solution was approximately [Ca] = 14 mM and [Al] = 26 mM. For preparation of the PVA organoceramic, atactic PVA (99.7% hydrolyzed, Polysciences, Warrington, PA) was dissolved in 5 mL of water and added to the calcium hydroxide solution. Solutions used to prepare the LDH were diluted with an equivalent amount of water to ensure identical ionic concentrations. Solid reaction products (LDH or PVA organoceramic) formed immediately upon mixing of the two ionic solutions ([PVA] = 100 mM), and were allowed to age in the mother liquor for 24–48 h. Solid products were isolated by centrifugation, washed with acetone, and dried in vacuo. The solids were ground to a powder, passed through a 100-mesh sieve and stored at 2 °C over $CaSO_4$. Elemental analysis of carbon and hydrogen were performed using a Control Equipment Corp. Model 240XA elemental analyzer. Ca and Al analyses were performed utilizing a Perkin-Elmer Model P2000 inductively coupled plasma emission sequential spectrophotometer.

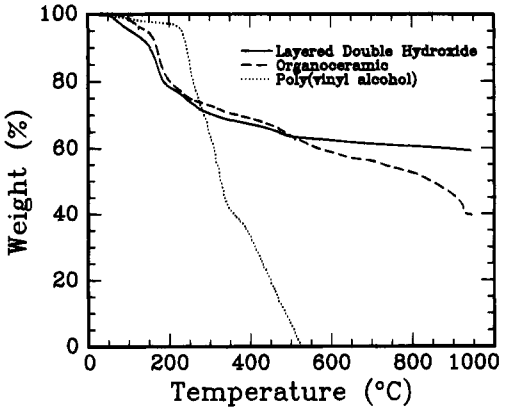

Figure 1. Thermogravimetric analysis of organoceramic, bulk poly(vinyl alcohol), and the pure layered double hydroxide $[Ca_2Al(OH)_6]^+[(OH)\cdot 3H_2O]^-$.

XRD of the organoceramic powders was performed on a Rigaku Geigerflex X-ray diffraction instrument (Rigaku USA, Inc., Danvers, MA) operating at 40 kV and 40 mA, with Ni-filtered Cu Kα radiation (λ = 1.54 Å). Powder samples were analyzed at scanning rates of 5–8° 2θ/min with a sampling interval of 0.04° 2θ and additively scanned 2–4 times in order to increase the signal-to-noise ratio. For analysis requiring accurate d spacings, samples were scanned at a rate of 1° 2θ/minute and a sampling interval of 0.01° 2θ.

For infrared analysis, disks containing 1–3 mg of sample and 0.3 g of KBr were mixed for 30 s in a grinder/mixer and then pressed in vacuo at 16 000 psi for 2 min in a Macro/Micro KBr Die (Spectra-Tech). The resulting disks, 13 mm in diameter by 1–2 mm thick, were transparent and were stored in a desiccator over $CaSO_4$ until analyzed. An IBM IR30 (IBM Corp., Danbury, CT) Fourier transform infrared spectrometer with a liquid nitrogen-cooled mercury cadmium telluride detector was used for all samples. Spectra of good signal-to-noise ratio were obtained from 100 scans at a resolution of 2 cm^{-1}. To minimize spectral absorbances due to atmospheric CO_2 and water, the sample compartment was purged with dry nitrogen for a minimum of 10 min before spectra were recorded. Reference spectra of pure KBr disks were recorded, stored, and digitally subtracted from sample spectra.

TGA of powders (20–50 mg) was conducted in flowing air at 60 cm^3/min using a DuPont 951 thermogravimetric analyzer at a constant heating rate of 10 °C per minute to a maximum of 1000 °C. For comparison, a powdered sample of bulk PVA was also tested. This polymer was the same used in the preparation of organoceramic powders and had a viscosity-average molecular weight of 60 100.

Samples were subjected to heat treatment at temperatures from 60 to 1000 °C. Sample powder (0.2–0.3 g) was put into a glass Petri dish and heated in air in an equilibrated muffle furnace (Fisher Isotemp) for 24 h. Thus, samples were immediately exposed to the required temperature and held at that temperature for 24 h. After heating for 24 h at the required temperature, samples were removed from the furnace and allowed to cool in a glass desiccator over P_2O_5. Following cooling to room temperature, samples were put in glass vials and stored desiccated at 2 °C in a refrigerator until analyzed by XRD, FTIR, and SEM. Gold-coated powder samples were imaged in the secondary electron mode at an accelerating voltage of 15–25 kV on a Hitachi S-800 scanning electron microscope.

Results and Discussion

TGA thermograms of the pure LDH $[Ca_2Al(OH)_6]^+[(OH)\cdot 3H_2O]^-$, the PVA organoceramic, and bulk PVA are shown in Figure 1. Below 500 °C, the thermogram for the PVA organoceramic is qualitatively similar to that of $[Ca_2Al(OH)_6]^+[(OH)\cdot 3H_2O]^-$, except that the curve is displaced slightly to higher temperatures

Table 1. Phases Detected by X-ray Diffraction after Heating the Layered Double Hydroxide and the PVA Organoceramic

temperature (°C)	layered double hydroxide	PVA organoceramic
60	$[Ca_2Al(OH)_6]^+[(OH)\cdot 3H_2O]^-$	layered nanocomposite[a]
80	$[Ca_2Al(OH)_6]^+[(OH)\cdot 3H_2O]^-$	layered nanocomposite
100	$[Ca_2Al(OH)_6]^+[(OH)\cdot 3H_2O]^-$	layered nanocomposite
125	$[Ca_2Al(OH)_6]^+[(OH)]^-$	layered nanocomposite
150	$[Ca_2Al(OH)_6]^+[(OH)]^-$	layered nanocomposite
175	$[Ca_2Al(OH)_6]^+[(OH)]^-$	layered nanocomposite
200	$Ca(OH)_2$	layered nanocomposite
250	$Ca(OH)_2$	layered nanocomposite
300	$Ca(OH)_2$	layered nanocomposite
400	$Ca(OH)_2 + CaCO_3$	layered nanocomposite
500	$CaCO_3$	$CaCO_3$
600	CaO	$CaCO_3$
700	$CaO + 12CaO\cdot 7Al_2O_3$	$CaO + CaCO_3$
800	$CaO + 12CaO\cdot 7Al_2O_3$	CaO + unknown phase
900	$CaO + 12CaO\cdot 7Al_2O_3$	$CaO + 12CaO\cdot 7Al_2O_3 + 3CaO\cdot Al_2O_3$
1000	$CaO + 12CaO\cdot 7Al_2O_3$	$CaO + 12CaO\cdot 7Al_2O_3 + 3CaO\cdot Al_2O_3$

[a] Layered nanocomposite refers to a structure in which the expanded layers of the PVA organoceramic are preserved after heating to the temperature indicated in the table.

throughout this temperature range. This shift indicates a slightly slower weight loss for the PVA organoceramic. In contrast to $[Ca_2Al(OH)_6]^+[(OH)\cdot 3H_2O]^-$, there was significant weight loss above 500 °C for the organoceramic, ending at roughly 900 °C. Interestingly, the decomposition of bulk PVA is complete at much lower temperatures (approximately 500 °C) than that of PVA contained in the organoceramic. As expected, the final mass after heating of the organoceramic is much lower than that of the LDH, reflecting the degradation of organic polymer initially present in the nanocomposite.

Chemical composition data obtained from organoceramic heated at various temperatures are shown in Figure 2, and the phases present in the powders, as identified by XRD, are shown in Table 1. The organoceramic used in this study contained 22.5% carbon which corresponds to 41% polymer by weight. As Figure 2 shows, the amount of carbon in the nanocomposite remains above 20% up to 200 °C. Above this temperature there is a gradual decrease in %C and little carbon remains at 800 °C. The gradual decrease in %H and increase in %Ca and %Al over the entire temperature range is attributed to the volatilization of water and low molecular weight organics formed during PVA degradation,[23] as well as the loss of water due to dehydration of the inorganic hydroxide phase.

The morphological changes accompanying the pyrolysis of the LDH and organoceramic powders are shown in Figures 3–6. As described previously[4] the spherical, multifaceted texture of the as-synthesized organoceramic particles is in stark contrast to the typical thin platelet morphology of the LDH. Particle morphology remained unchanged below 300 °C in both the PVA organoceramic and $[Ca_2Al(OH)_6]^+[(OH)\cdot 3H_2O]^-$ powders (see Figure 3). At 300 °C (Figure 4) small crystals of $Ca(OH)_2$ were observed on the surface of the remnant plates of $[Ca_2Al(OH)_6]^+[(OH)\cdot 3H_2O]^-$. The identification of these crystals as $Ca(OH)_2$ was made through XRD scans and the FTIR spectrum. At 500 °C (Figure 5) crystals of $CaCO_3$ were detected on the surface of the $[Ca_2Al(OH)_6]^+[(OH)\cdot 3H_2O]^-$ plates. XRD and FTIR analysis were also used to identify these crystals. Most importantly, no morphological changes were observed when organoceramic particles were heated to 800 °C. However, heating of the organoceramic to 1000 °C resulted in apparently solid spherical particles (Figure 6), instead of the multifaceted and porous (Figure 3) organoceramic particles from which they derived.

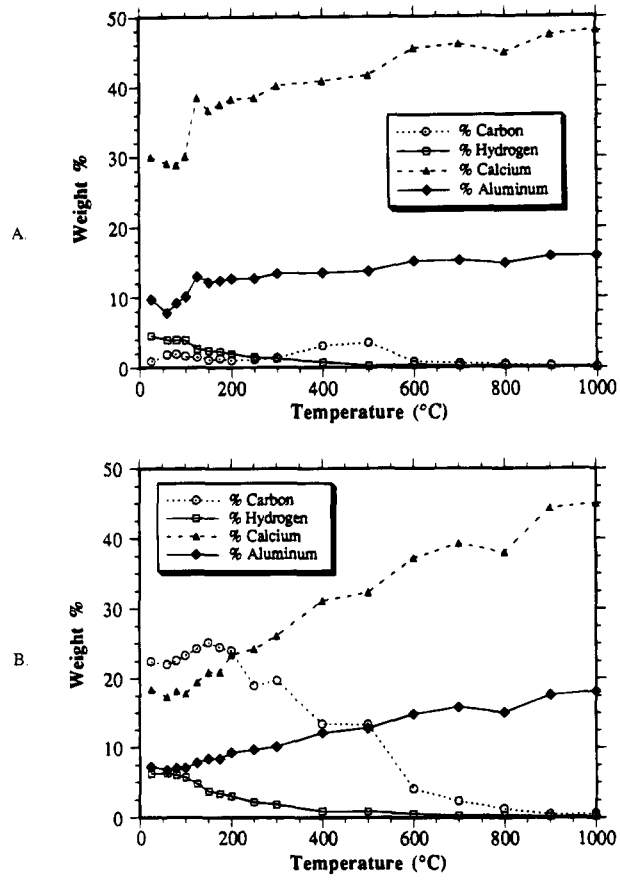

Figure 2. Chemical composition of the layered double hydroxide powder (A) and organoceramic (B) heated to the temperatures indicated.

Thermal decomposition of the PVA organoceramic involves presumably mechanisms in which degradation of inorganic layers and of intercalated and adsorbed PVA are coupled. Thus, we first consider the chemical, structural, and morphological changes occurring in the pure LDH during heating. LDHs are a class of layered inorganic hydroxides which consist of planar divalent and trivalent metal hydroxide octahedral sheets separated by interlayers containing anions and water. Their thermal behavior has been thoroughly studied. Be-

(23) Miyata, S.; Kumura, T. *Chem. Lett.* **1973**, 843.

(24) Miyata, S. *Clays Clay Miner.* **1975**, *23*, 369.

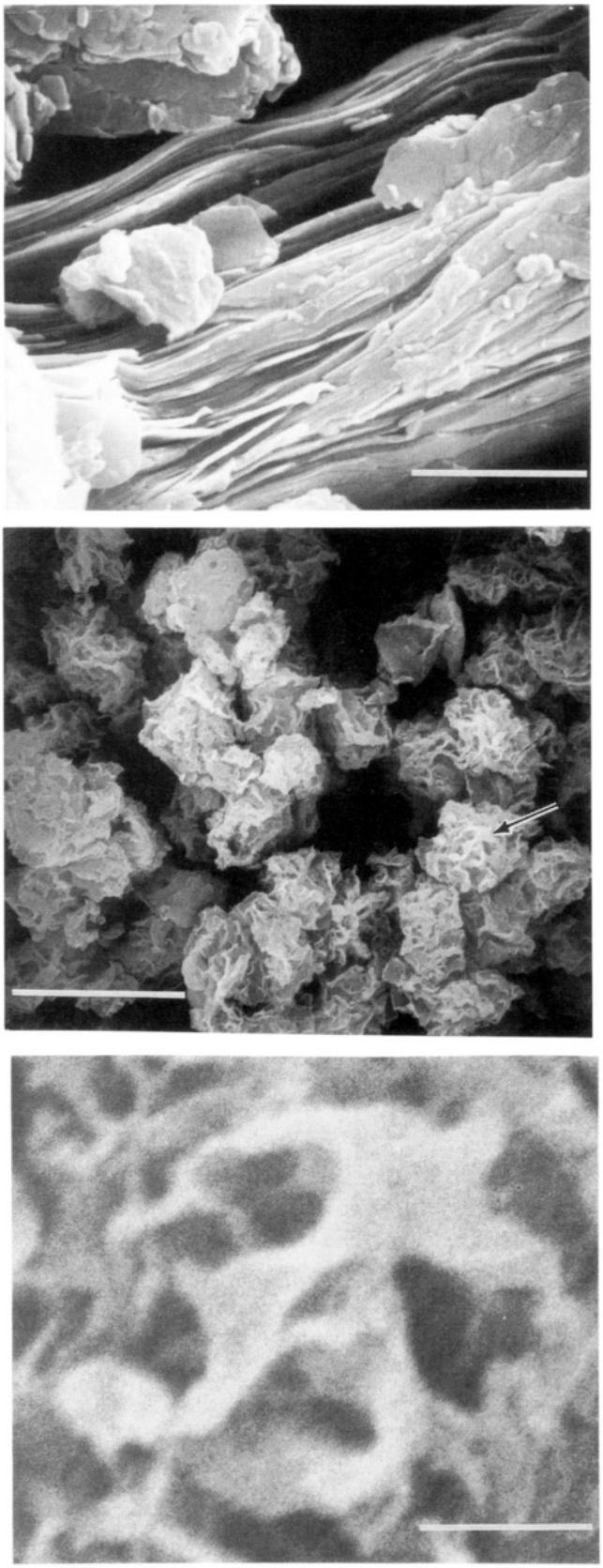

Figure 3. SEM micrographs of the as-synthesized powders of the layered double hydroxide (top) and organoceramic (middle). The magnification bars in the top and middle micrographs correspond to 1 and 10 μm, respectively. The bottom micrograph is an enlargement of the area marked with an arrow in the middle micrograph, and its magnification bar corresponds to 1 μm. A comparison between the top and bottom micrographs reveals clearly the morphological difference between layered double hydroxide and organoceramic.

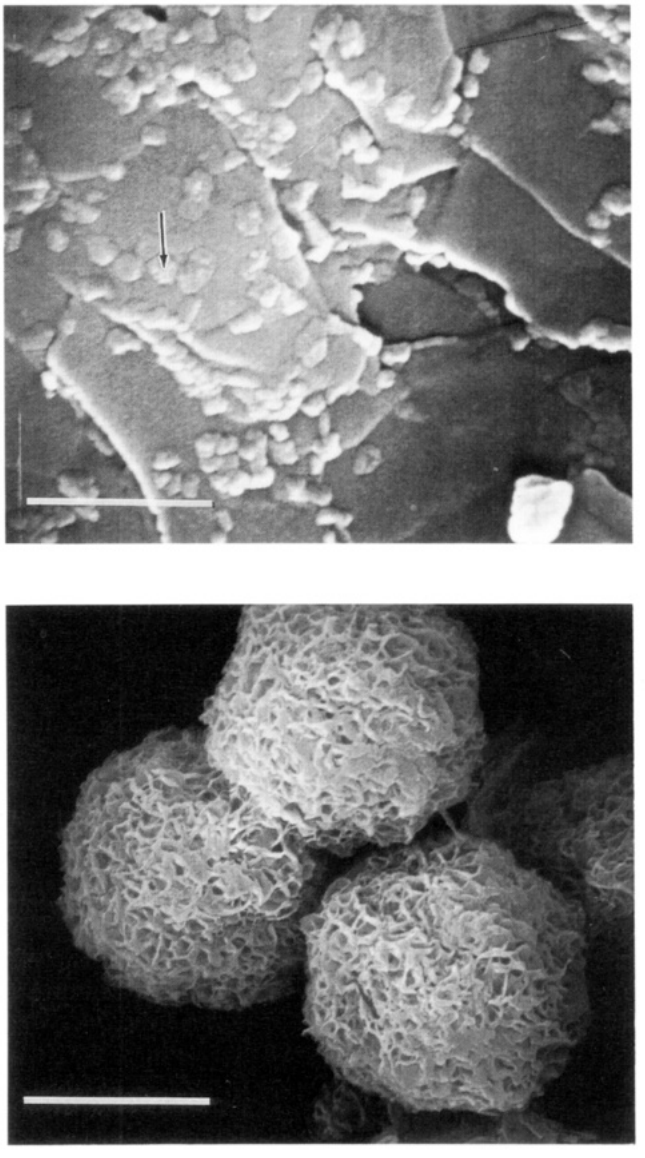

Figure 4. SEM micrographs of the layered double hydroxide (top) and organoceramic (bottom) heated to 300 °C for 24 h. The magnification bars in the top and bottom micrographs correspond to 5 and 2.31 μm, respectively. Arrows in the top micrograph indicate the locations of $Ca(OH)_2$ crystals.

tween room temperature and approximately 200 °C there is a rapid loss of weight corresponding to removal of water harbored in the interlayers. This behavior is typical of most LDHs, although composition may affect the temperature range within which water loss occurs.[23,24] At this point the material is presumably of composition $[Ca_2Al(OH)_6]^+[OH]^-$ corresponding to a weight loss of 19.3%. A second distinct region of decomposition occurs between 200 and 500 °C and corresponds primarily to formation of metal hydroxides as octahedral LDH layers decompose. This decomposition also liberates water, formed by condensation of octahedrally coordinated OH^- ions. XRD (Table 1), FTIR (Figure 7), and SEM (Figure 4) indicate the presence of crystalline $Ca(OH)_2$ in this temperature range. An amorphous $Al(OH)_3$ phase might also be present since crystalline phases containing Al are only detected above 500 °C. Between 400 and 600 °C $CaCO_3$ crystals are observed on the surface of the LDH particles (see Figure 5) and accounts for the slight increase in %C observed between 400 and 600 °C (Figure 2). The source of carbon for carbonate formation should be CO_2

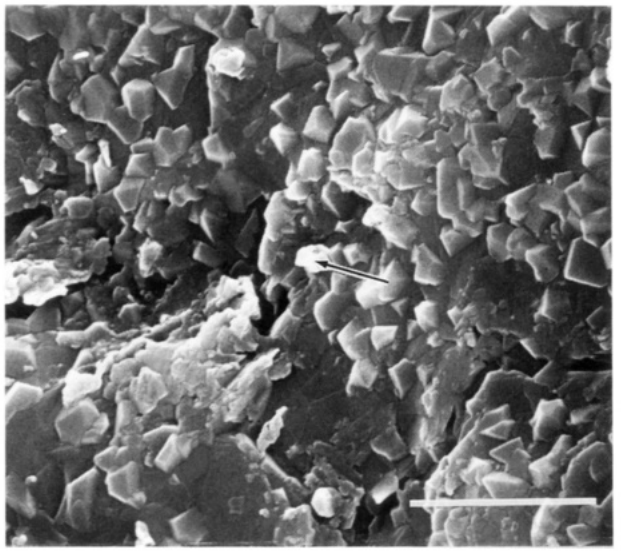

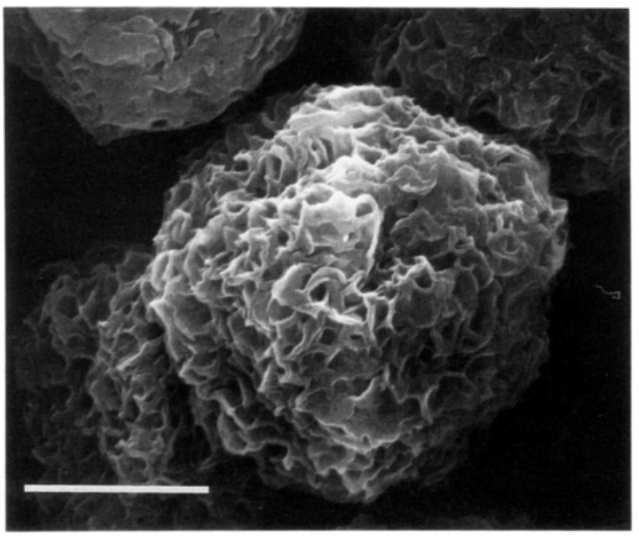

Figure 5. SEM micrographs of the layered double hydroxide (top) and organoceramic (bottom) heated to 500 °C for 24 h. The magnification bars in the top and bottom micrographs correspond to 1.5 μm. The arrow in the top micrograph points to a $Ca(CO_3)$ crystal.

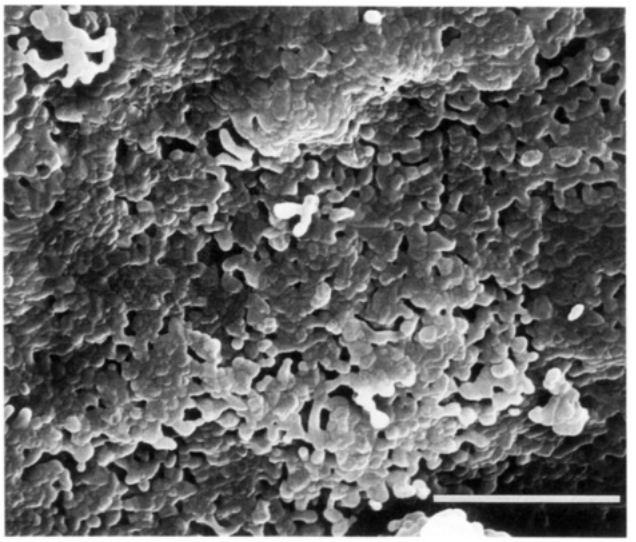

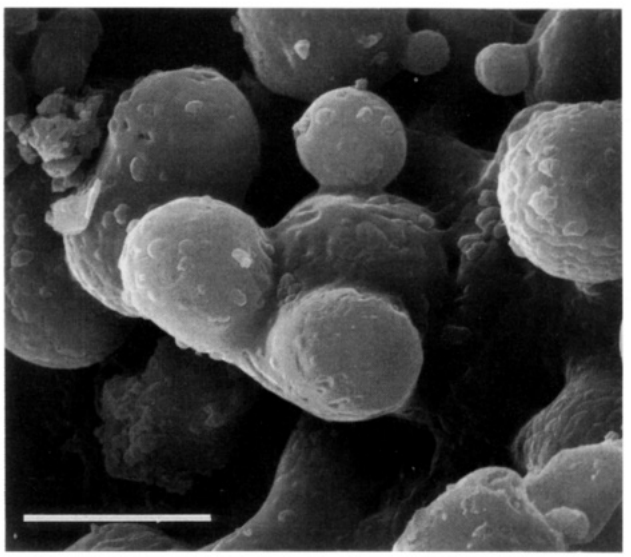

Figure 6. SEM micrographs of the layered double hydroxide (top) and organoceramic (bottom) heated to 1000 °C for 24 h. The magnification bars in the top and bottom micrographs correspond to 3 and 2.7 μm, respectively.

from the atmosphere, as no attempt was made to exclude it from the atmosphere. At temperatures above 500 °C there is relatively little weight loss, with formation and maturation of crystalline Ca and Al oxides such as CaO and $12CaO{\cdot}7Al_2O_3$.

The changes observed in LDH particles linked to decomposition of inorganic layers were found to be suppressed in the organoceramic. Following heating of the organoceramic to 300 °C, infrared bands characteristic of the calcium aluminate disappear and are replaced by a strong, broad O−H stretching band (3430 cm^{-1}) assigned to PVA (based on comparison with the spectrum of bulk PVA), possibly with some contribution from amorphous hydroxide phases (Figure 7). Notably absent from the OH stretching region is the sharp peak at 3646 cm^{-1} seen in the spectrum of the LDH powder heated to 300 °C. This peak is attributed to crystalline $Ca(OH)_2$,[25] and its absence is in agreement with the absence of crystalline $Ca(OH)_2$ in the XRD pattern of the organoceramic. $Ca(OH)_2$ is normally the first phase to be produced as a result of decomposition of $[Ca_2Al(OH)_6]^+[(OH)\cdot 3H_2O]^-$ principal layers. Formation of $Ca(OH)_2$ crystals requires large-scale rearrangement (diffusion) of cations and hydroxide ions. Their formation could be prevented by the presence of strong hydrogen bonding between PVA or PVA degradation products and OH^- ions or water molecules in the principal layer. This could prevent or delay large-scale diffusion of ions that is necessary for the formation of crystalline $Ca(OH)_2$. The broad, featureless OH stretching absorption observed in the organoceramic heated to 300 °C (Figure 7) is consistent with the prevention of $Ca(OH)_2$ crystallization and the formation of an amorphous Ca- and Al-containing hydroxide phase that is engaged in hydrogen bonding to hydroxyl groups on the PVA chain.

It is unclear from the data at what point the PVA has completely degraded, although between 200 and 800 °C there is a gradual loss of carbon indicating the continuous degradation of PVA, perhaps resulting in formation of water, aldehydes, carbon monoxide, and aromatic hydrocarbons.[21] Starting at low temperature (~100 °C) one observes the disappearance of the PVA C−O stretch

(25) Henning, O. In *The Infrared Spectra of Minerals*; Farmer, V. C., Ed.; Mineralogical Society: London, 1974; pp 445−463.

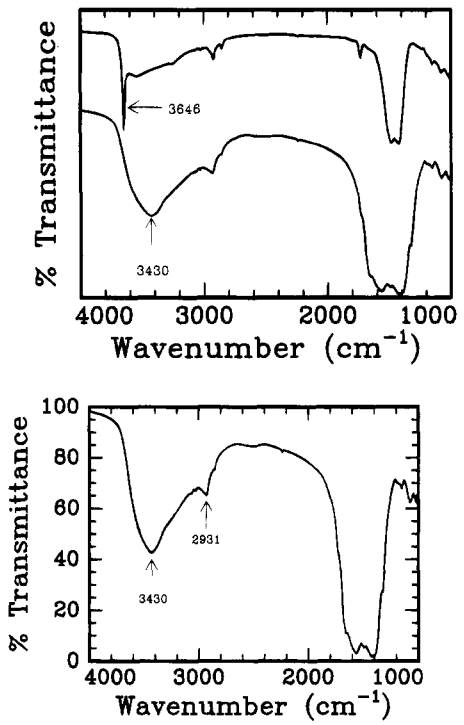

Figure 7. FTIR spectra of the layered double hydroxide (top) and organoceramic (bottom) powders heated to 300 °C for 24 h.

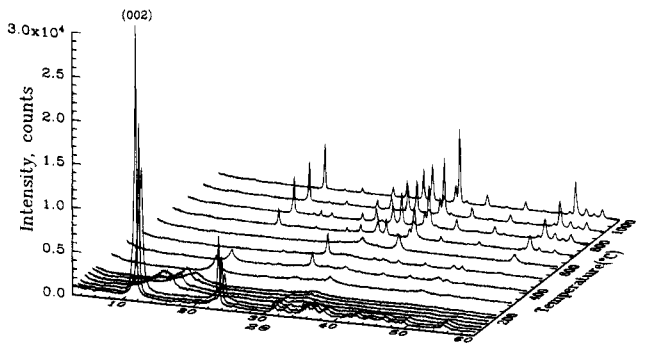

Figure 8. 3-D plot of powder X-ray diffraction patterns of the layered double hydroxide heated to various temperatures. The temperature range covered by the plot shown is 60–1000 °C. Phase compositions are described in Table 1.

at 1098 cm^{-1} which is replaced by broad and strong absorbances between 1580 and 1700 cm^{-1}, consistent with formation of carbonyl groups, alkene double bonds, and possibly also carboxyl groups. Also, there is a gradual reduction in the PVA O–H and CH_2 stretching absorptions above 200 °C. These changes are indicative of the dehydration of PVA, which involves the formation of carbonyl groups at an intermediate stage in the reaction[21]

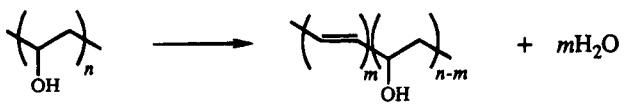

XRD patterns taken at various temperatures following heating of the pure LDH and the PVA organoceramic are shown in Figures 8 and 9, respectively. The crystalline phases present at various temperatures after heating of the LDH and PVA organoceramic were identified from the XRD data and are listed in Table 1. The broad first-order reflection labeled (002)* in Figure 9 corrresponds to the interlayer repeat distance (~18

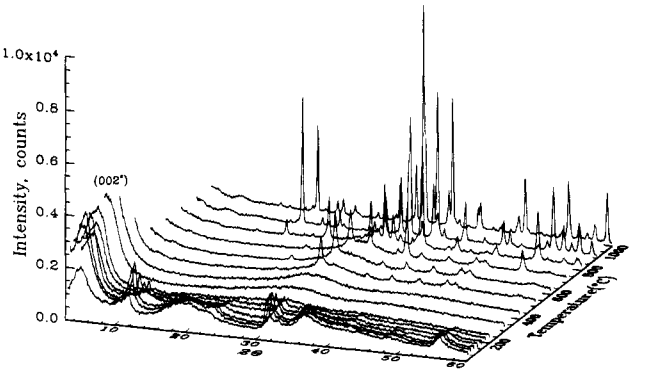

Figure 9. 3-D plot of powder X-ray diffraction patterns of organoceramic heated to various temperatures. The temperature range covered by the plot is 60–1000 °C. Phase compositions are described in Table 1.

Å) which represents a significant modification of the typical crystal structure of $[Ca_2Al(OH)_6]^+[(OH)\cdot 3H_2O]^-$.[4,5] This expanded layer spacing is observed at temperatures up to 400 °C. In contrast, the layered structure of the pure LDH is lost at approximately 125 °C (Figure 8). Above 500 °C, both materials transform to a mixture of oxide phases including CaO and $12CaO\cdot 7Al_2O_3$. However, the PVA organoceramic heated above 900 °C was found to contain $3CaO\cdot Al_2O_3$, a phase not observed in the LDH heated to the same temperature.

As mentioned above we observed the persistence of the expanded layer structure of the organoceramic at least up to 400 °C. This is quite remarkable considering the layered structure of the pure LDH thermally decomposes by 125 °C. The enhanced thermal stability of the organoceramic is most likely related to the intimate dispersion of polymer between the LDH principal layers. It is reasonable to suggest that bonds, possibly secondary, between the polymer (PVA or dehydrated PVA at higher temperatures) and the inorganic crystal, are responsible for the observed behavior. We have shown previously that the 10 Å expansion of the interlayer in the organoceramic corresponds to roughly two molecular layers of strongly adsorbed PVA chains.[4] The surfaces of the LDH layers are composed of hydroxide ions and water, providing a high concentration of potential sites for hydrogen bonding with PVA. In fact, PVA itself is also capable of acting as both donor and acceptor of hydrogen bonds. Thus, the extremely large area of bonding contact between the polymer and the inorganic crystal in the nanocomposite structure appears to have controlled the course of decomposition of the inorganic phase.

Conclusions

The presence of intercalated polymer retards the decomposition of the inorganic nanolayers of a calcium–aluminum layered double hydroxide and prevents formation of crystalline hydroxide phases at high temperatures. The polymer also leads to the formation of a high temperature oxide phase not observed during heating of the purely inorganic system. The prevention of hydroxide crystallization is possibly caused by the intimate bonding contact between inorganic crystal layers and the intercalated polymer. The course of thermal decomposition in the composite material is thus controlled by the extensive and intimately bonded interface area created by the nanoscale architecture of the organoceramic.

Acknowledgment. The authors gratefully acknowledge the support of this research by the Air force Office of Scientific Research through Grant AFOSR 90-0242. This project was part of the research program of the University of Illinois Center for Cement Composite Materials. We gratefully acknowledge the use of the Center's facilities as well as useful discussions with Professor J. F. Young.

CM940206X